

Elastic electron scattering and rovibrational excitation of N₂ at low incident energies

M J Brennan, D T Alle, P Euripides†, S J Buckman and M J Brunger†

Electron Physics Group, Atomic and Molecular Physics Laboratories, Research School of Physical Sciences and Engineering, Australian National University, Canberra, ACT 2601, Australia

Received 18 December 1991, in final form 24 March 1992

Abstract. The scattering of low energy electrons from nitrogen has been investigated for a range of impact energies (1.5, 2.1, 3.0 and 5.0 eV) which encompass the $^2\Pi_g$ resonance. Measured differential and integral cross sections for both elastic scattering and rovibrational excitation ($v=0-1, 2, 3$) of the ground electronic state are compared with results from previous experimental and theoretical investigations. In some cases, particularly at 1.5 eV, significant discrepancies are found between the present and previous experiments.

1. Introduction

Nitrogen is a natural target for studies of low energy electron–molecule scattering. The basic data arising from such studies are used, for example, in the modelling of important discharge-based technological processes. Perhaps more importantly, from a theoretical point of view, the nitrogen molecule has become almost a standard test case for low energy electron scattering calculations, particularly those that attempt to describe the scattering process in the region of a shape resonance. Molecular nitrogen is sufficiently aspherical and has an electronic structure which is sufficiently complicated to make it typical of small molecules with closed shells, while still remaining a computationally tractable target for electron scattering calculations. In many respects nitrogen is a better test case for scattering calculations than the next simplest commonly occurring molecule, hydrogen, as its 14 electrons make it more suitable for approximations such as the free-electron-gas approach to exchange. On the other hand its much smaller rotational constant reduces the importance of other approximations, such as the adiabatic nuclei approximation. However the representation of the nuclear dynamics remains important in describing elastic scattering and, in particular, vibrational excitation, in the vicinity of the $^2\Pi_g$ shape resonance (~ 2.4 eV).

Despite the extensive number of investigations, both experimental and theoretical, of low energy electron scattering from nitrogen there remain some discrepancies between experiment and theory. Surprisingly, there have been few absolute differential cross section measurements carried out in the energy region below the shape resonance but those that exist (Sohn *et al* 1986, Shyn and Carignan 1980, both at 1.5 eV), are generally about a factor of two lower than available calculations for elastic scattering.

† Present address: School of Physical Sciences, Flinders University of South Australia, Bedford Park, SA 5042, Australia.

At other energies there have been absolute differential cross section measurements by Tanaka *et al* (1981), Brunger *et al* (1989) and Srivastava *et al* (1976) although, with the possible exception of the $v=0-1$ process, insufficient experimental data are available to provide a definitive test of theory. The measurements presented here of absolute differential cross sections for elastic scattering and rovibrational excitation of nitrogen ($v=0-1, 2, 3$) have been conducted over a range of impact energies (1.5, 2.1, 3.0, 5.0 eV). These specific energies were chosen in order to provide an overlap with the results of other investigators and to test the available theory at energies where the resonance contribution to the cross section is both small (1.5 and 5.0 eV) and large (2.1 and 3.0 eV). In particular we make an extensive comparison with the hybrid theory calculation of Chandra and Temkin (1976). Other theoretical work relevant to the present study includes the multiple scattering method of Siegel *et al* (1978), the Schwinger multichannel calculation of Huo *et al* (1987), the *R*-matrix calculation of Gillan *et al* (1987) and the close coupling calculations of Morrison *et al* (1987).

We have also extrapolated the experimental results to 0° and 180° and integrated the resultant differential cross section to obtain total elastic, total vibrational and grand total cross sections. The latter, in particular, can be compared with a substantial body of accurate, absolute integral cross section measurements from attenuation experiments (e.g. Baldwin 1974, Kennerly 1980, Jost *et al* 1983).

In the following section the experimental apparatus and the procedures that we have employed for the present measurements are outlined. In section 3 the experimental results are presented, together with the work of other investigators, and a critical comparison is made of both experiment and theory. This is followed by some concluding remarks.

2. Experimental apparatus and procedures

The electron monochromator employed in the present measurements, and its principles of operation, have been described in detail previously by Brunger *et al* (1990, 1991). Briefly, a beam of N_2 effusing from a multichannel capillary array is crossed with a beam of monoenergetic electrons of desired energy E_0 . Vibrationally elastic (henceforth referred to as 'elastic') and inelastically scattered electrons are energy analysed and detected as a function of scattering angle. The true scattered signal is the difference between the intensity recorded when the gas beam is admitted to the chamber via the capillary array (signal+background) and the intensity recorded when the gas is admitted to the chamber, at the same rate, via another capillary located at the periphery of the chamber (background). The energy resolution in the present measurements (typically 60 meV) was sufficient to resolve the rotationally summed vibrational (henceforth called rovibrational) transitions of interest from each other and from the elastically scattered electrons. A typical energy loss spectrum which illustrates this point is shown in figure 1.

The scattered electron analyser can be rotated about the molecular beam axis allowing access to an angular range of -20° to 130° . The true 0° position was determined as that about which the intensity of elastically scattered electrons, and/or those producing rovibrational excitation, was symmetric. The estimated error in this determination was $\pm 1^\circ$. As the energy regime of the present work encompasses the well known $^2\Pi_g$ resonance, and the elastic and rovibrational cross sections vary quite sharply as a function of the incident electron beam energy (see for example Chandra and Temkin

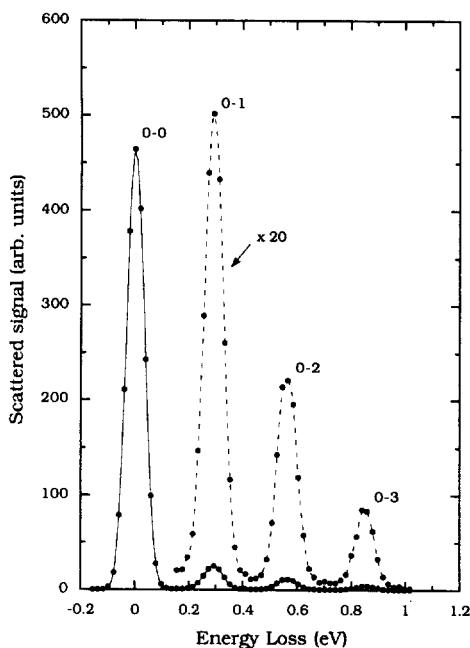


Figure 1. Electron energy loss spectrum for N_2 at an incident energy of 3.0 eV and a scattering angle of 30° . The inelastic transitions have been scaled by a factor of 20.

1976), particular attention was paid to the energy calibration of the incident electron beam. This was done by detecting, in the elastic channel, both the 2^2S resonance in helium at 19.367 eV and the $2^2\Sigma_g^+$ resonance in N_2 at 11.480 eV, at a number of different scattering angles. The energy scales established for each gas agreed with each other to within 20 meV and we estimate that the absolute energy scale for the present measurements is reliable to within 50 meV.

As in our previous study of the $e^- + H_2$ collision system (Brunger *et al* 1990, 1991, Buckman *et al* 1990) the absolute scale of the elastic N_2 collision cross section, at a given E_0 , was determined by the relative flow technique (Nickel *et al* 1989). This technique required a separate series of experiments in which the respective relative flow rates of helium and molecular nitrogen into the scattering chamber were measured as a function of the driving pressure behind the capillary. The technique used in these measurements is very similar to that of Khakoo and Trajmar (1986) and so we do not go into further detail here. The results of the present calibration for N_2 and He are given in figure 2, where the normalized flow rates (the measured relative flow rates multiplied by the square root of the respective molecular masses) are plotted as a function of the capillary driving pressure. The driving pressure was measured by an MKS Baratron capacitance manometer. In addition, the driving pressures were carefully adjusted for each scattering measurement so that the mean free path for each gas at the entrance of the capillary array was identical. Under these circumstances the elastic cross section for molecular nitrogen is related to that for helium via:

$$\frac{d\sigma}{d\Omega}(\theta)_{N_2} = \frac{I_{He}}{I_{N_2}} \frac{N_e(\theta)_{N_2}}{N_e(\theta)_{He}} \frac{P_{He}}{P_{N_2}} \frac{d\sigma}{d\Omega}(\theta)_{He} \quad (1)$$

where P are the capillary driving pressures for each gas, I the electron beam currents,

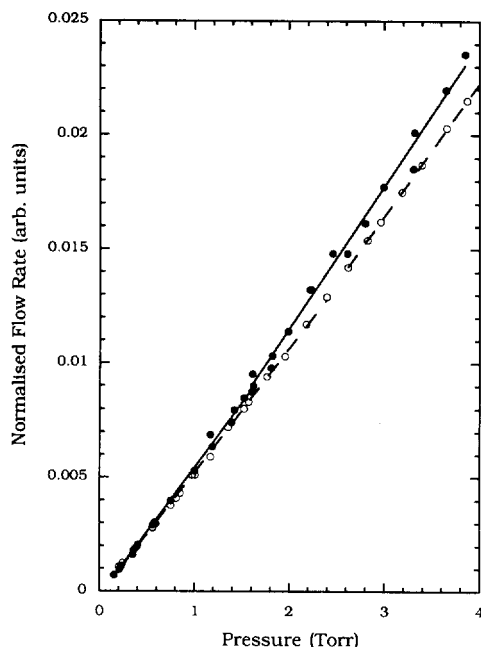


Figure 2. Normalized flow rates (see text) for helium (○) and N_2 (●) as a function of the capillary driving pressure.

$N_e(\theta)$ the scattered electron count rates and $d\sigma/d\Omega(\theta)_{He}$ the known elastic cross section for helium obtained from the *ab initio* variational calculation of Nesbet (1979).

The differential cross sections for the rovibrational excitation processes were then obtained at each energy and scattering angle via analysis of the measured energy loss spectra. In the present case this yielded the ratio of the integrated intensity of the rovibrational feature of interest (up to $v=3$) to the integrated elastic intensity, that is:

$$R_v(E_0, \theta) = \frac{N_v(E_0, \theta)}{N_0(E_0, \theta)} \quad v = 1, 2, 3 \quad (2)$$

where N_v and N_0 are the true signal levels for rovibrational excitation and elastic scattering respectively. Provided possible sources of systematic error in the experiment such as (i) transmission effects associated with the analyser electron optics, (ii) stray electric or magnetic fields, and (iii) angle-dependent effects associated with the analyser have been adequately dealt with (see Brunger *et al* 1990, 1991) then $R_v(E_0, \theta)$ is related to the differential cross sections of the relevant scattering processes via:

$$R_v(E_0, \theta) = \frac{\sigma_v(E_0, \theta)}{\sigma_0(E_0, \theta)}. \quad (3)$$

Hence the required rovibrational differential cross sections could be determined by multiplying the relevant ratio at each scattering angle by the appropriate differential cross section for elastic scattering at that same angle.

Having obtained the elastic and rovibrational differential cross sections, they were then extrapolated to 0° and 180° by using the shape of the available theoretical cross sections as a guide. These (measured plus extrapolated) cross sections were then integrated to give the total elastic, total rovibrational and grand total cross sections.

The problems associated with this extrapolation procedure have been discussed in some detail by Brunger *et al* (1991) and whilst we do not reiterate them here we do point out that they are almost certainly more important now than in the earlier H_2 work, which did not exhibit much structure in the measured differential cross sections.

3. Results and discussion

3.1. Elastic scattering

The present differential cross sections for elastic scattering are given in table 1 and shown in figure 3(a)–(d). The estimated absolute uncertainty in these measurements is $\pm 8\%$. Several previous measurements and calculations of elastic scattering are available for comparison in the energy range covered by the present measurements. At 1.5 eV (figure 3(a)) the agreement between the present data and those of both Sohn *et al* (1986) and Shyn and Carignan (1980) is poor, the present cross section being almost universally a factor of two higher than the others, although the agreement with respect to the shape of the angular distributions is quite good, particularly with the measurement of Sohn *et al*. The obvious reason for this discrepancy lies in the absolute normalization of the relative angular distributions. However, this is somewhat puzzling, particularly in the case of Sohn *et al*, as their data were also placed on an absolute scale by the use of the relative flow technique and the helium cross section. The present data are in better agreement with the various calculations available at this energy. These include the hybrid calculation of Chandra and Temkin (1976), which is in good accord with both the shape and magnitude of the present data over the whole angular range, the Schwinger multichannel calculation of Huo *et al* (1987) and the model potential calculation of Morrison *et al* (1987). We shall return to a broader discussion of this experimental discrepancy later.

At higher energies the level of agreement with other experimental investigations is somewhat improved. At 2.1 eV (figure 3(b)) the present data are in excellent accord

Table 1. Differential elastic scattering cross sections for N_2 ($10^{-16} \text{ cm}^2 \text{ sr}^{-1}$) at incident energies between 1.5 and 5.0 eV.

θ (deg)	E_0 (eV)			
	1.5	2.1	3.0	5.0
15	0.567	—	—	—
20	0.646	2.96	3.89	1.86
30	0.648	2.12	3.47	1.90
40	0.837	1.63	2.95	1.78
50	1.18	1.49	2.19	1.47
60	1.33	1.51	1.49	1.16
70	1.42	1.52	1.11	0.905
80	1.47	1.47	0.872	0.685
90	1.28	1.22	0.751	0.577
100	1.16	1.04	0.701	0.546
110	1.02	0.900	0.708	0.521
120	0.889	0.911	0.774	0.533
130	0.669	1.05	0.987	0.552

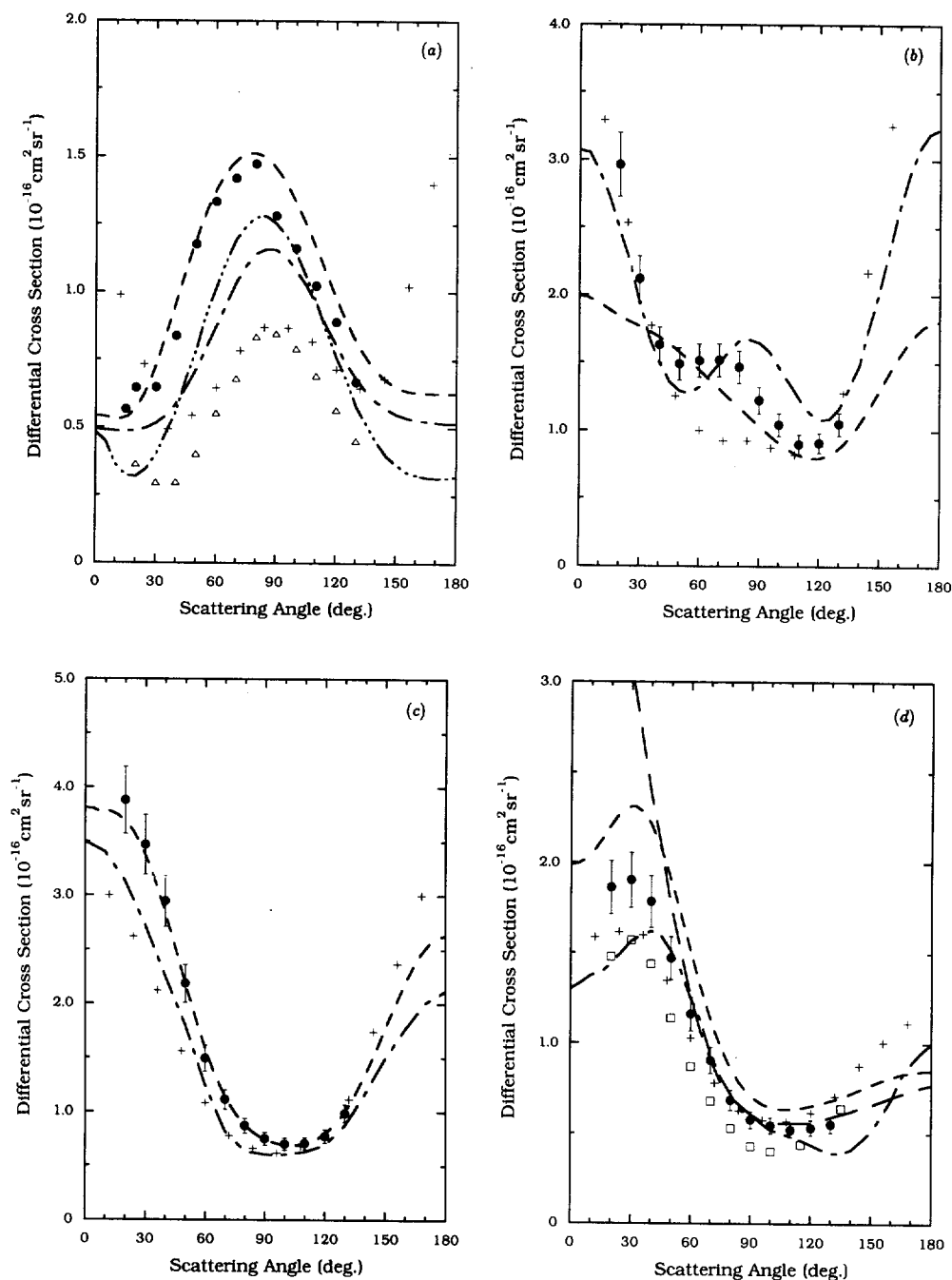


Figure 3. Differential elastic scattering cross section at (a) 1.5 eV, (b) 2.1 eV, (c) 3.0 eV, (d) 5.0 eV in units of $10^{-16} \text{ cm}^2 \text{ sr}^{-1}$. ●, present results; +, Shyn and Carignan; △, Sohn *et al*; □, Srivastava *et al*; ----, Chandra and Temkin; -.-.-, Huo *et al*; —, Gillan *et al*; ·····, Morrison *et al*.

with the elastic cross section of Shyn and Carignan at both forward and backward angles but there are substantive discrepancies in the mid-angular range (50 – 100°) where the present cross section is about 50% larger and displays a pronounced structure which is not evident in the data of Shyn and Carignan. As we have discussed in the previous section, this discrepancy may in part be due to a slight difference in the energy calibration between the two experiments. For example, a strong energy dependence in the shape of the differential cross section is evident in the hybrid theory calculations at energies of 2.1 and 2.3 eV. The present result at this energy is in reasonably good agreement with the cross section of Huo *et al*, who also find a structure at mid angles, whilst the comparison with the hybrid theory calculation of Chandra and Temkin is not as favourable as at 1.5 eV. At 3.0 eV (figure 3(c)) the present differential cross section shows the same general form as that measured by Shyn and Carignan although the present cross section is 30–40% higher for scattering angles less than about 80° . Once again the present data are in excellent agreement with the hybrid theory calculation of Chandra and Temkin whilst the calculation of Huo *et al* is in slightly better accord with the measurement of Shyn and Carignan. However we stress that the conclusions which can be drawn from comparisons in this energy region (2.1 and 3.0 eV) are limited due to the strong energy dependence of the cross section.

At 5.0 eV (figure 3(d)) we once again observe a reasonable level of agreement with the experiment of Shyn and Carignan as well as with that of Srivastava *et al* (1976) although there are discrepancies of the order of 20% between all three data sets over various parts of the angular range. In particular, at forward angles, the present cross section is higher than both other measurements and also the calculation of Huo *et al* but lower than the hybrid theory cross section. Indeed the shape of the present cross section is in excellent agreement with Chandra and Temkin's but about 15% lower over the whole angular range. There is also an *R*-matrix calculation available at this energy (Gillan *et al* 1987) which appears to be much too large at forward angles but is in good agreement with the present data at angles greater than 60° .

3.2. Rovibrational excitation

The differential cross sections for rovibrational excitation are given in tables 2, 3 and 4 and shown in figures 4, 5 and 6 for the $v=0$ –1, 2, 3 excitations respectively. The estimated absolute uncertainty in these cross sections is ± 15 , ± 17 and $\pm 18\%$ respectively. Note that the excitation of the $v=0$ –2, 3 bands has only been measured at 2.1 and 3.0 eV in the present study. At all energies, and for all rovibrational excitations studied, the present differential cross sections exhibit the same general shape with minima at around 60 and 120° and a secondary maximum at about 90° . This of course is characteristic of dominant d-wave scattering and it reflects the importance that the $N_2^- \ ^2\Pi_g$ resonance plays in vibrational excitation N_2 at these energies.

Several other experimental cross sections are available for comparison with the present measurement for the $v=0$ –1 excitation. At 1.5 eV (figure 4(a)) the present cross section shows some difference in *shape* to that of Sohn *et al* (1986), unlike the situation that pertained to elastic scattering where the discrepancies were in the absolute magnitude of the cross section. At scattering angles less than about 50° the two cross sections agree within the error bars but, for larger scattering angles, the present cross section is about a factor of two larger. It is possible that this shape difference is a manifestation of an energy calibration difference between the two experiments although such an effect should not be too marked at this energy, which is outside the region of

Table 2. Differential cross sections for rovibrational excitation ($v=0-1$) of N_2 ($10^{-18} \text{ cm}^2 \text{ sr}^{-1}$) at incident energies between 1.5 and 5.0 eV.

θ (deg)	E_0 (eV)			
	1.5	2.1	3.0	5.0
5	—	84.6	41.7	2.03
10	—	70.5	37.2	1.91
15	1.68	—	—	—
20	1.42	51.0	30.0	1.52
30	1.09	29.8	21.9	1.05
40	0.773	15.0	13.6	0.733
50	0.527	11.2	9.12	0.526
60	0.579	10.5	6.41	0.409
70	0.643	13.5	7.23	0.546
80	0.671	14.2	9.12	0.597
90	0.708	12.4	9.80	0.609
100	0.635	10.8	8.72	0.496
110	0.565	8.43	7.48	0.394
120	0.503	7.54	5.91	0.306
130	—	8.70	5.56	0.377

Table 3. Differential cross sections for rovibrational excitation ($v=0-2$) of N_2 ($10^{-18} \text{ cm}^2 \text{ sr}^{-1}$) at incident energies of 2.1 and 3.0 eV.

θ (deg)	E_0 (eV)	
	2.1	3.0
5	48.1	20.5
10	41.6	18.9
20	27.9	15.2
30	17.8	10.5
40	10.4	7.39
50	6.75	4.94
60	7.47	4.29
70	8.46	5.58
80	9.16	6.81
90	8.67	7.27
100	7.37	6.86
110	5.84	5.91
120	5.69	4.68
130	6.90	4.07

strong influence of the resonance. The hybrid theory cross section is symmetric about 90° (as it is for all rovibrational excitations), and as such does not reproduce the enhanced forward scattering observed experimentally. At 2.1 eV (figure 4(b)), we make a comparison with the experimental cross section of Brunger *et al* (1989) and note that, whilst there is good agreement in the shapes of the two cross sections, the present measurement is about 20–30% lower than their cross section over their angular range of 20 to 90° . With the exception of very forward scattering angles, it is also lower than the hybrid theory calculation (by about a factor of two at 90°). At 3.0 eV (figure 4(c))

Table 4. Differential cross sections for rovibrational excitation ($v=0-3$) of N_2 ($10^{-18} \text{ cm}^2 \text{ sr}^{-1}$) at incident energies of 2.1 and 3.0 eV.

θ (deg)	E_0 (eV)	
	2.1	3.0
5	11.0	5.56
10	9.50	5.38
20	6.60	4.32
30	4.10	3.76
40	2.51	2.51
50	1.71	1.45
60	1.82	1.08
70	2.37	1.53
80	2.44	1.81
90	2.23	2.13
100	1.66	1.77
110	1.50	1.59
120	1.62	1.16
130	1.75	1.16

several other experiments and calculations are available for comparison. Again the cross section of Brunger *et al* is somewhat larger than the present at angles greater than 60° but is in better agreement at forward angles. The cross section of Tanaka *et al* (1981) is slightly flatter than the present measurement, being about 30% lower at 20° and 20% higher at 90° , but the overall agreement in shape and absolute magnitude is reasonably good. The hybrid theory calculation is in good agreement with the present measurement for scattering angles greater than 30° whilst the *R*-matrix cross section shows excellent shape agreement but is consistently 20–50% higher than the present measurements. Finally at 5.0 eV (figure 4(d)), we find a good level of agreement between the present results and those of Tanaka *et al* and also with the hybrid theory and *R*-matrix calculations, with the former lying closer to the experimental data.

For the higher vibrations, which have been studied at 2.1 and 3.0 eV, only one other experiment, that of Brunger *et al* (1989), and two calculations, those of Chandra and Temkin and Gillan *et al*, are available for comparison. For the $v=0-2$ excitation we find good agreement with the experimental data of Brunger *et al* at 2.1 eV (figure 5(a)), whilst at 3.0 eV (figure 5(b)) the agreement (within combined error bars) is confined to the angular range above about 40° . An interesting contrast is seen in the comparison with the hybrid theory calculation. At 2.1 eV (figure 5(a)), this theory is about a factor of two higher than the present experiment over the whole angular range, whilst at 3.0 eV (figure 5(b)), it is about four times smaller than the present data. At 3.0 eV the *R*-matrix calculation also appears to underestimate the cross section. For the $v=0-3$ excitation, there is good agreement between the two experiments at both energies for scattering angles less than 60° but there are some substantial discrepancies ($\approx 100\%$) between the present results and those of Brunger *et al* at larger angles. At both energies the hybrid theory is substantially larger than experiment and, at 3.0 eV in particular, the theory is about a factor of four larger than the present experiment. The *R*-matrix cross section, at an energy of 3.0 eV, also clearly overestimates the excitation of this channel. Whilst the above remarks are based on the observed behaviour in figure 5 we should, once again, emphasize that the strong energy dependence in the

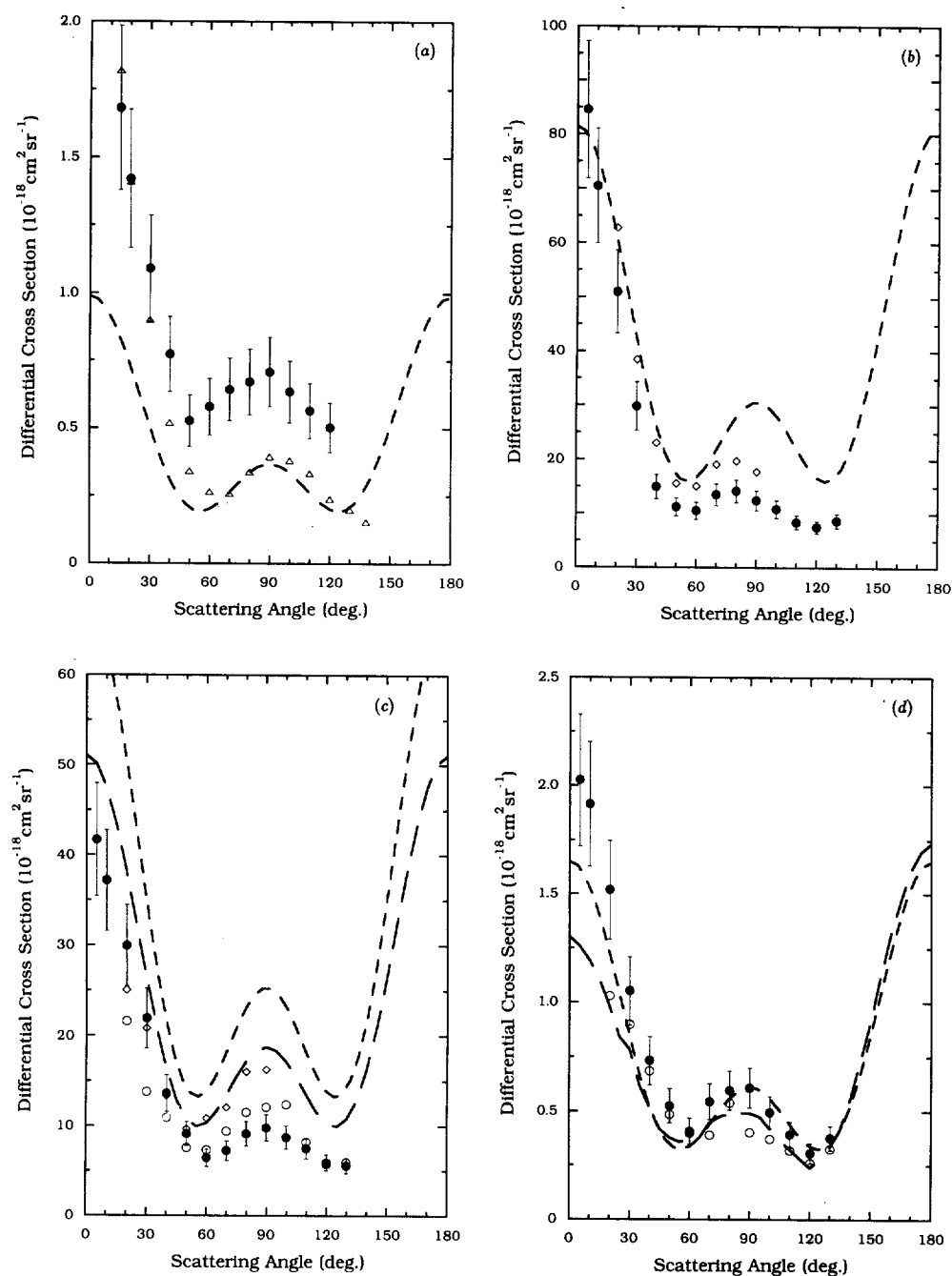


Figure 4. Differential rovibrational ($v=0-1$) scattering cross section at (a) 1.5 eV, (b) 2.1 eV, (c) 3.0 eV, (d) 5.0 eV in units of $10^{-18} \text{ cm}^2 \text{ sr}^{-1}$. ●, present results; △, Sohn *et al*; ◇, Brunger *et al*; ○, Tanaka *et al*; ---, Chandra and Temkin; —, Gillan *et al*.

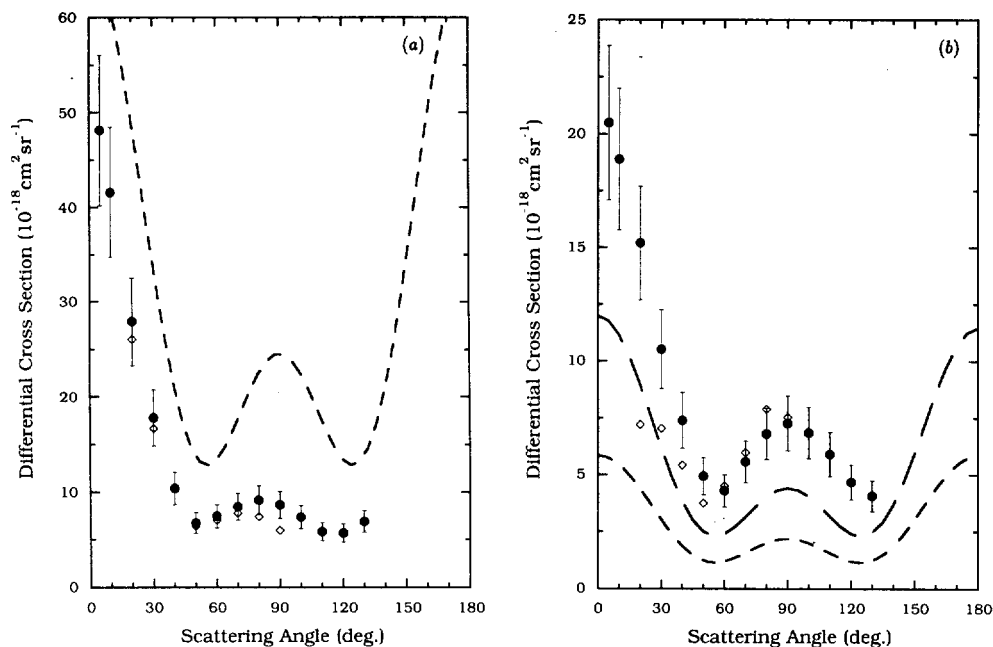


Figure 5. Differential rovibrational ($v=0-2$) scattering cross section at (a) 2.1 eV, (b) 3.0 eV, in units of $10^{-18} \text{ cm}^2 \text{ sr}^{-1}$. ●, present results; ◇, Brunger *et al.*; ---, Chandra and Temkin; —, Gillan *et al.*

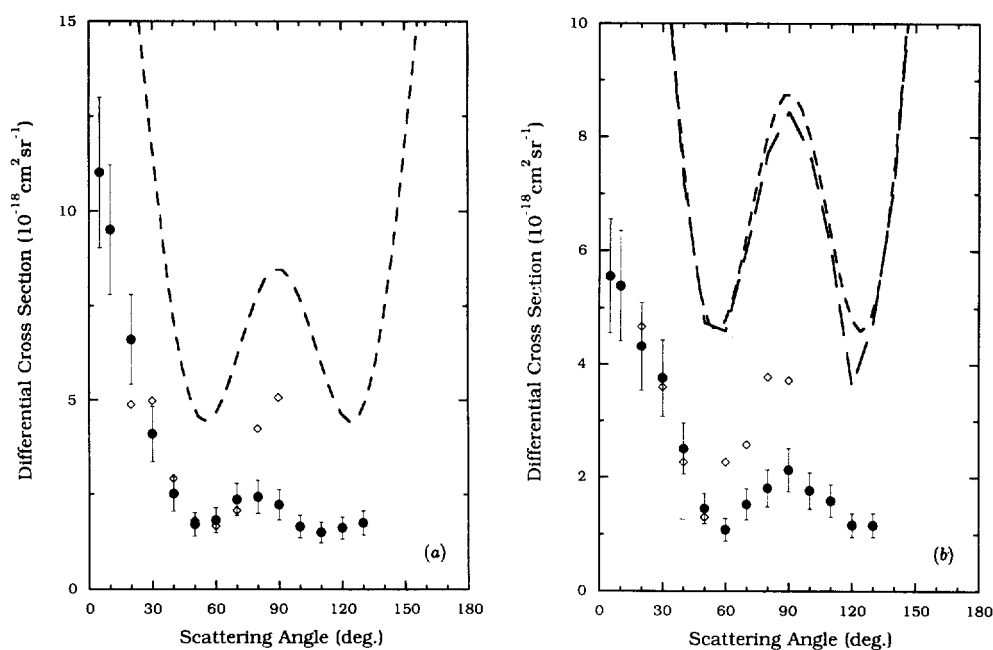


Figure 6. Differential rovibrational ($v=0-3$) scattering cross section at (a) 2.1 eV, (b) 3.0 eV, in units of $10^{-18} \text{ cm}^2 \text{ sr}^{-1}$. ●, present results; ◇, Brunger *et al.*; ---, Chandra and Temkin; —, Gillan *et al.*

resonance region is also observed in the higher vibrational cross sections (e.g. Ehrhardt and Willmann 1967, Boness and Schulz 1973, Allan 1985) and it is possible that some, or all, of the discrepancies between the measured and calculated cross sections may be due to small energy calibration differences.

One may further speculate that the discrepancy at middle angles between the present data and those of Brunger *et al* (1989) for the excitation of the $v=0-1, 3$ vibrational states at 2.1 and 3.0 eV and the good agreement shown with these measurements for the $v=0-2$ excitation at these energies, is also due to small differences in energy between the two experiments that manifest themselves as substantive differences in the absolute magnitude of the measured differential cross sections.

3.3. Integral cross sections

The differential cross sections discussed above have been extrapolated and integrated to provide total elastic, total vibrational and grand total cross sections at each of the energies investigated. Whilst it should be stressed that, particularly in the case of the grand total cross section, there are more accurate methods to obtain such cross sections than via integrating differential measurements, such a procedure does allow a comparison to be made with accurate measurements that are available from techniques such as time-of-flight attenuation experiments and, as we attempt to point out here, such a comparison is helpful in assessing the accuracy of the differential measurements.

The extrapolation has been carried out using the calculations of Chandra and Temkin as a guide to the shape of the cross section in the region where we have not performed measurements. In general this procedure is based on the reasonable level of agreement which is found in the shape of the measured and calculated cross sections. The only exception to this occurs for elastic scattering at 2.1 eV where the present measurement is quite different in shape to the calculation of Chandra and Temkin. In this case the theory of Huo *et al* (1987) was used for the extrapolation. It is difficult to accurately assess the uncertainty that arises from the extrapolation procedure but, as an example, the contribution of the extrapolated values to the integrand varied between 7.8% ($v=0-0$ at 1.5 eV) to a worst case of 23.2% ($v=0-1$ also at 1.5 eV). If we assume an uncertainty of $\pm 20\%$ in the extrapolation this results in an overall uncertainty of at most $\pm 25\%$ in the integral cross sections.

The total elastic, total vibrational, and grand total cross sections are presented in table 5. We also present, for the purposes of comparison, the grand total cross sections of Kennerly (1980) obtained by a time-of-flight technique. The agreement between the

Table 5. Total elastic, total vibrational and grand total cross sections for N_2 (10^{-16} cm^2).

Process	Energy (eV)			
	1.5	2.1	3.0	5.0
$0 \rightarrow 0$	12.7	18.4	18.7	11.3
$0 \rightarrow 1$	0.089	1.97	1.37	0.080
$0 \rightarrow 2$	—	1.32	0.90	—
$0 \rightarrow 3$	—	0.34	0.26	—
Grand total	12.8	22.0	21.2	11.4
Kennerly (1980)	11.24	24.13	19.73	11.60

present grand total cross sections and those of Kennerly is excellent at all the energies of the present study. In particular, at 1.5 eV where there is such a marked difference between the absolute value of the present differential cross section and those of both Sohn *et al* (1986) and Shyn and Carignan (1980), the present grand total cross section is 14% higher than that of Kennerly, but within our experimental uncertainty. In contrast, the published total elastic cross sections of Sohn *et al* (7.43 \AA^2) and Shyn and Carignan (9.6 \AA^2) (which account for more than 99% of the grand total cross section at this energy), are considerably lower than the accepted value from attenuation experiments. Whilst some of this difference in the integrated cross section may result from uncertainties in the extrapolation to forward and backward angles, this cannot be the sole cause of the problem and it may be indicative of a normalization problem in these measurements.

For the integral rovibrational cross sections there is, to our knowledge, only one other tabulated absolute cross section with which we can compare. At an incident energy of 3.0 eV the value measured by Tanaka *et al* (1981) for the $v=0-1$ transition, 1.23 \AA^2 , is in good agreement with the present value of 1.37 \AA^2 .

4. Conclusions

The present measurements of elastic scattering and rovibrational excitation at 1.5, 2.1, 3.0 and 5.0 eV provide a body of absolute differential cross section data against which previous experiments and theory can be compared. In particular, they provide information for higher vibrational excitations over a much larger angular range than has previously been measured. In general, the agreement between the present measurements and previous experiments is reasonable although there are some notable exceptions. The most serious discrepancy arises for elastic scattering at 1.5 eV where the present cross section is about a factor of two higher than previous measurements. Comparisons of total cross sections derived from each of the experiments with accurate values from attenuation experiments indicate a possible normalization problem in the previous measurements.

We have also compared the results of the present experiments with several theoretical calculations which employ quite different approaches to the scattering problem. In particular, the extensive set of cross sections available from the hybrid theory approach of Chandra and Temkin has enabled us to chart its success or otherwise, both as a function of energy and vibrational quanta, in the region of the $^2\Pi_g$ resonance. In general all of the calculations against which we have compared show a reasonable agreement with the present experiments for both the shape and magnitude of the differential cross sections for elastic scattering. For vibrational excitation there is no regular pattern that emerges from the comparison of theory and experiment and whilst the overall trends are similar there are only a few cases where the apparent level of agreement could be described as good, $v=0-1$ at 3.0 eV (*R*-matrix calculation) and 5.0 eV (hybrid theory calculation) for example. In particular the calculations do not agree with the experiment on the relative strengths of each vibrational excitation at any given energy. For example, at 3.0 eV, the hybrid theory calculation shows excellent agreement with the experiment in the shape of both the $v=0-2$ and $v=0-3$ cross sections but for the former it is a factor of four smaller than experiment whilst for the latter it is a factor of four larger. However we reiterate that small differences in energy calibration can lead to substantial differences in the cross section at both 2.1 and 3.0 eV

and, as a result, great care must be exercised in assessing the level of agreement with both other experiments and with theory.

Acknowledgments

We would like to thank Michael Morrison who, in the course of many extended conversations concerning electron-diatomic molecule scattering, suggested this project; Grahame Danby for many useful discussions; Aaron Temkin for providing tabulated values of scattering coefficients from which the hybrid theory results presented in this paper were calculated; Robert Gulley for assistance with the preparation of some of the plots and Malcolm Elford and Paul Burrow for comments on the manuscript. M J Brunger wishes to thank the Rothmans Education Foundation for the provision of a Fellowship during the course of this work.

References

- Allan M 1985 *J. Phys. B: At. Mol. Phys.* **18** 4511
Baldwin G C 1974 *Phys. Rev. A* **9** 1225
Boness M J W and Schulz G J 1973 *Phys. Rev. A* **8** 2883
Brunger M J, Buckman S J and Newman D S 1990 *Aust. J. Phys.* **43** 665
Brunger M J, Buckman S J, Newman D S and Alle D T 1991 *J. Phys. B: At. Mol. Opt. Phys.* **24** 1435
Brunger M J, Teubner P J O, Weigold A M and Buckman S J 1989 *J. Phys. B: At. Mol. Opt. Phys.* **22** 1443
Buckman S J, Brunger M J, Newman D S, Snitchler G, Alston S, Norcross D W, Morrison M A, Saha B C, Danby G and Trail W K 1990 *Phys. Rev. Lett.* **65** 3253
Chandra N and Temkin A 1976 *Phys. Rev. A* **13** 188
— 1976 *NASA Technical Note D-8547*
Ehrhardt H and Willmann K 1967 *Z. Phys.* **204** 462
Gillan C J, Nagy O, Burke P G, Morgan L A and Noble C J 1987 *J. Phys. B: At. Mol. Phys.* **20** 4585
Huo W M, Lima M A P, Gibson T L and McKoy V 1987 *Phys. Rev. A* **36** 1642
Jost K, Bisling P G F, Eschen F, Felsmann M and Walther L 1983 *Proc. 13th Int. Conf. on the Physics of Electronic and Atomic Collisions (Berlin)* ed J Eichler et al (Amsterdam: North-Holland) Abstracts p 91
Khakoo M A and Trajmar S 1986 *Phys. Rev. A* **34** 138
Kennerly R E 1980 *Phys. Rev. A* **21** 1876
Morrison M A, Saha B C and Gibson T L 1987 *Phys. Rev. A* **36** 3682
Nesbet R K 1979 *Phys. Rev. A* **20** 58
Nickel J C, Zetner P W, Shen G and Trajmar S 1989 *J. Phys. E: Sci. Instrum.* **22** 730
Shyn T W and Carignan G R 1980 *Phys. Rev. A* **22** 923
Siegel J, Dill D and Dehmer J L 1978 *Phys. Rev. A* **17** 2106
Sohn W, Kochem K-H, Scheuerlein K-M, Jung K and Ehrhardt H 1986 *J. Phys. B: At. Mol. Phys.* **19** 4017
Srivastava S K, Chutjian A and Trajmar S 1976 *J. Chem. Phys.* **63** 2659
Tanaka H, Yamamoto T and Okada T 1981 *J. Phys. B: At. Mol. Phys.* **14** 2081